Universal Two-Step Approach to Degradable and Electroactive Block Copolymers and Networks from Combined Ring-Opening Polymerization and Post-Functionalization via Oxidative Couplin...

ARTICLE *in* MACROMOLECULES · JULY 2011

Impact Factor: 5.8 · DOI: 10.1021/ma2009595

3 AUTHORS:

Baolin Guo
Xi'an Jiaotong University
41 PUBLICATIONS **652** CITATIONS
SEE PROFILE

Anna Finne-Wistrand
KTH Royal Institute of Technology
86 PUBLICATIONS **1,392** CITATIONS
SEE PROFILE

Ann-Christine Albertsson
KTH Royal Institute of Technology
419 PUBLICATIONS **11,374** CITATIONS
SEE PROFILE

Macromolecules

ARTICLE

pubs.acs.org/Macromolecules

Universal Two-Step Approach to Degradable and Electroactive Block Copolymers and Networks from Combined Ring-Opening Polymerization and Post-Functionalization via Oxidative Coupling Reactions

Baolin Guo, Anna Finne-Wistrand, and Ann-Christine Albertsson*

Department of Fibre and Polymer Technology, School of Chemical Science and Engineering, Royal Institute of Technology, SE-100 44, Stockholm, Sweden

Supporting Information

ABSTRACT: We present a universal strategy for the facile synthesis of degradable and electroactive block copolymers and organogels (DEBCGs) based on aniline oligomers and polyesters in a two-step approach, here exemplified by the preparation of a series of DECBCGs based on aniline tetramer (AT) and poly(ε-caprolactone) (PCL). Polyesters with an aniline dimer (AD) segment were first obtained by controlled ring-opening polymerization (ROP) of ε-caprolactone initiated by the amine group of AD with or without 2,2-bis(ε-caprolactone-4-yl) propane (BCP). The postpolymerization modification via an oxidative coupling reaction between AD and a polyester was then used to form the electroactive segment AT in the copolymers or organogels. The molecular weight and conductivity of the block copolymers and organogels were controlled by the AT content. The chemical structure, electroactivity, and thermal properties of DEBCGs were investigated by FT-IR, NMR, SEC, UV, cyclic voltammetry, TGA, and DSC. Our general strategy for the synthesis of DECBCGs avoids the multiple step reactions and low efficiency involved in previous work.

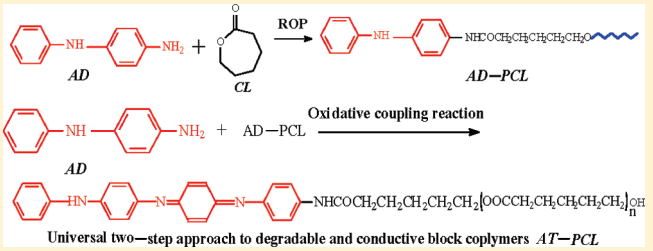

INTRODUCTION

Aliphatic polyesters such as polylactones and polylactide are the candidates in biomedical and pharmaceutical applications because of their excellent biocompatibility, biodegradability, and mechanical properties.[1,2] Polyesters with tailored structures and properties are usually synthesized by ring-opening polymerization initiated by an alcohol or amine with a catalyst.[3−6] Functionalization of polyesters will greatly extend their application in the biomedical field.[7−10] An easy and effective way to introduce functional groups into the polyesters is to use initiators with specific functional groups.[11−13] These functional groups can be used for covalently attaching biomacromolecules or drugs, for postmodification, and for tuning the hydrophilicity of the polyesters.[14,15]

The development of biodegradable biomaterials has reached such a level that the biomaterials, once implanted, will induce specific cellular responses at the molecular level.[16] Electrical stimulation has been proved to be able to tune a range of cellular activities.[17,18] Degradable and electrically conductive polymers (DECPs) represent a new class of biomaterials and have been attracting great attention. Langer et al[19] introduced carboxyl groups as side groups of polypyrrole, so that the conductive polymers can undergo slow water erosion due to the hydrophilic nature of the polymers. Schmidt et al[20,21] connected the oligothiophene and oligopyrrole with ester linkages, and the polymers obtained had good biocompatibility. Wei et al[22,23] synthesized linear triblock and multiblock DECPs using the coupling reaction between aniline pentamer and polylactide. Zhang et al[24,25] linked aniline pentamer to the main chain of polyphosphazene to obtain DECPs. We expanded the macromolecular architecture of DECPs, and synthesized star-shaped[26] and hyperbranched[27] degradable conductive copolymers based on polylactide, polycaprolactone, aniline trimer and aniline pentamer. Furthermore, degradable and electroactive hydrogels which combine the special properties of degradable hydrogels such as their rubbery nature similar to soft tissues, their easy control of diffusivity of small molecules, and their excellent biocompatibility, and conductive polymers having unique advantages of electroactivity, optical switching and electrical properties have been developed by our group.[28−30] A series of degradable and conductive hydrogels with tunable electrical conductivities and tunable swelling behavior have been successfully synthesized and fully characterized. These hydrogels were composed of acrylated poly(D,L-lactide)−poly(ethylene glycol)−poly(D,L-lactide), glycidyl−methacrylate-functionalized polycaprolactone−poly(ethylene glycol)−polycaprolactone, aniline tetramer, and aniline pentamer using photopolymerization and coupling reactions.[28,29]

Received: April 27, 2011
Revised: June 1, 2011
Published: June 15, 2011

dx.doi.org/10.1021/ma2009595 | *Macromolecules* 2011, 44, 5227–5236

Table 1. Feed Ratio of the Degradable and Electroactive Block Copolymers and Organogels

sample code	AD (mg)	CL (mg)	$Sn(Oct)_2$ (mg)	AD−PCL or AD−BCP−PCL (mg)	$(NH_4)_2S_2O_8$ (mg)	BCP (mg)
AD7.5−PCL	75	925	3			
AD10−PCL	100	900	3			
AD15−PCL	150	850	3			
AD20−PCL	200	800	3			
AT7.5−PCL	75			1000	186	
AT10−PCL	100			1000	248	
AT15−PCL	150			1000	372	
AT20−PCL	200			1000	496	
AD7.5−BCP−PCL	75	810	3			115
AD10−BCP−PCL	100	743	3			157
AD15−BCP−PCL	150	619	3			231
AD20−BCP−PCL	200	487	3			313
AT7.5−BCP−PCL	75			1000	186	
AT10−BCP−PCL	100			1000	248	
AT15−BCP−PCL	150			1000	372	
AT20−BCP−PCL	200			1000	496	

Reviewing the synthesis of all the degradable and electrically conductive polymers and hydrogels (DECPHs), we found that the strategy for synthesizing DECPHs in all the previous work was to combine the conductive segments (such as oligopyrrole,[19] oligothiophene,[20,21] and oligoaniline,[22−32]) and degradable segments (such as linear polylactide,[22,23,28] star-shaped polylactide,[26] PCL,[27,29] polyglycolide,[31] polyphosphazene,[24,25] and chitosan[30,32]) together into one macromolecule or network. However, this strategy usually involves multiple step reaction, tedious purification, and low efficiency and in some cases also toxic reagents and a low yield. We have developed a two-step synthesis for degradable and conductive hydrogels based on chitosan and aniline tetramer,[30] but chitosan as a natural polymer may lead to an undesirable immune response and batch-to-batch variation because of the inability to control techniques during processing. In contrast, polyesters usually have a well-defined structure and customer-made properties. The goal is a universal two-step approach for the easy synthesis of degradable and electroactive block copolymers and organogels based on polyesters and aniline oligomers. Aniline dimer (AD) is a starting material for the synthesis of aniline tetramer (AT), and it contains an amine group. We hypothesize that the AD could be used as an initiator for ring-opening polymerization of lactones and lactides (such as lactide, ε-caprolactone, glycolide, 1,5-dioxepan-2-one, and so on) to obtain a well-defined structured polyester with AD segment. Oxidative coupling functionalization between AD and the AD segment in the polyester could be used for the second step to form an electroactive AT segment. AT from the degradation process of the copolymers might be consumed by macrophages and could undergo renal clearance, avoiding long-term adverse effect in vivo.[19,20] Consequently, degradable and electroactive block copolymers and organogels with well-defined structure can be obtained in a simple two step reaction. Using this synthesis strategy, we synthesized a series of AT−PCL block copolymers and organogels with different molecular weights and different AT contents. Their structures and properties were also investigated.

EXPERIMENTAL SECTION

Materials. Monomer ε-caprolactone (CL, purity: 99%) (Aldrich) was dried over CaH_2 for 48 h, and then distilled under reduced pressure. Stannous octoate, $Sn(Oct)_2$ (Sigma-Aldrich, Sweden) was dried over molecular sieves prior to use. *N*-Phenyl-1,4-phenylenediamine (aniline dimer, AD), ammonium persulfate ($(NH4)_2S_2O_8$), ammonium hydroxide (NH_4OH), hydrochloric acid (HCl), dimethylformamide (DMF), and dimethyl sulfoxide (DMSO) were all purchased from Aldrich and used as received.

2,2-Bis(ε-caprolactone-4-yl) propane (BCP) was synthesized according to the procedure in the literature.[33,34] The white powder obtained was finally recrystallized from acetone and dried under reduced pressure. ^{1}H NMR (400 MHz, $CDCl_3$, ppm): 4.34 (R, R), 4.15 (S, R) (t, 2H, $-CH_2OOC-$), 2.72 (R, R), 2.56 (S, R) (t, 2H, $-CH_2COO-$), 1.95 (q, 2H, $-CH_2-C-OOC-$), 1.59 (q, 2H, $-CH_2-CH_2-COO-$), 1.40 (m, 1H, $-CH_2-CH-CH_2-$), 0.79 (t, 3H, $-CH_3$). These data agree well with our previous results.[33,34]

Synthesis of AD−PCL. Polyesters AD−PCL were obtained by ring-opening polymerization of CL in bulk with aniline dimer (AD) as initiator. The monomer (CL), initiator (AD), and co-initiator ($Sn(Oct)_2$) were weighed and added to the flask in a glovebox (Mbraun MB 150B-G-I) purged with nitrogen (Table 1). The mixture was then immersed in an oil bath at 110 °C under a nitrogen atmosphere for 48 h. The theoretical contents of AD in the polyester were set as 7.5%, 10%, 15%, and 20%. The molar ratio of CL to $Sn(Oct)_2$ was 1000:1. After the reaction, 20 mL chloroform was added to the flask to dissolve the polymer, which was then precipitated in 300 mL hexane/methanol (v:v = 95:5) solution. The product was dried in a vacuum oven at room temperature for 48 h after filtration. Samples were coded as AD7.5−PCL, AD10−PCL, AD15−PCL, and AD20−PCL, which means that the AD−PCL block copolymers contain 7.5%, 10%, 15%, and 20% weight ratio of AD in the copolymer, respectively. The synthesis route is shown in Scheme 1. ^{1}H NMR (400 MHz, DMSO-d_6): 9.70 (s, 1H, $-CO-NH-$), 7.99 (s, 1H, $-NH-$), 7.44 (d, 2H, Ar−H), 7.17 (t, 2H, Ar−H), 7.06 (m, 4H, Ar−H), 6.76 (m, 1H, Ar−H), 4.36 (t, 2H, $-CO-CH_2-$), 3.98 (m, 2H, $-O-CH_2-$), 2.27 (m, 2H, $-CH_2-$), 1.50 (m, 2H, $-CH_2-$), 1.28 (m, 2H, $-CH_2-$).

Synthesis of AT−PCL. The AT−PCL block copolymer was synthesized by the coupling reaction between AD and AD−PCL shown in Scheme 1. In the synthesis of AT10−PCL for example, 1000 mg AD10−PCL and 100 mg AD were dissolved in 5 mL DMF and 10 mL acetone mixture, and 10 mL 1 mol/L HCL was then added into the solution. 248 mg $(NH_4)_2S_2O_8$ was dissolved in 5 mL distilled water, and then added to the mixture drop by drop in 20 min. The mixture became

Scheme 1. Synthesis of Degradable and Electroactive Block Copolymers in a Two-Step Process

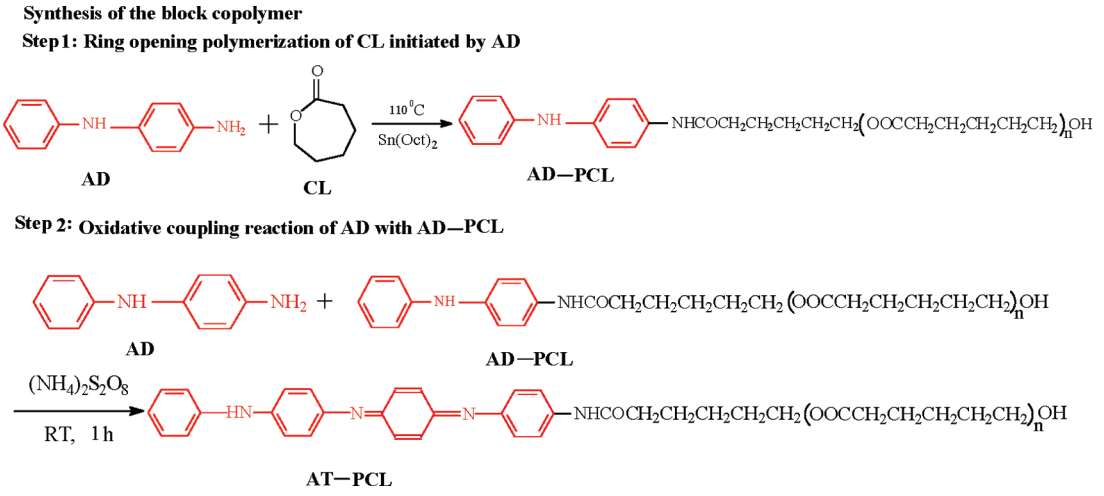

Scheme 2. Synthesis of Degradable and Electroactive Organogels

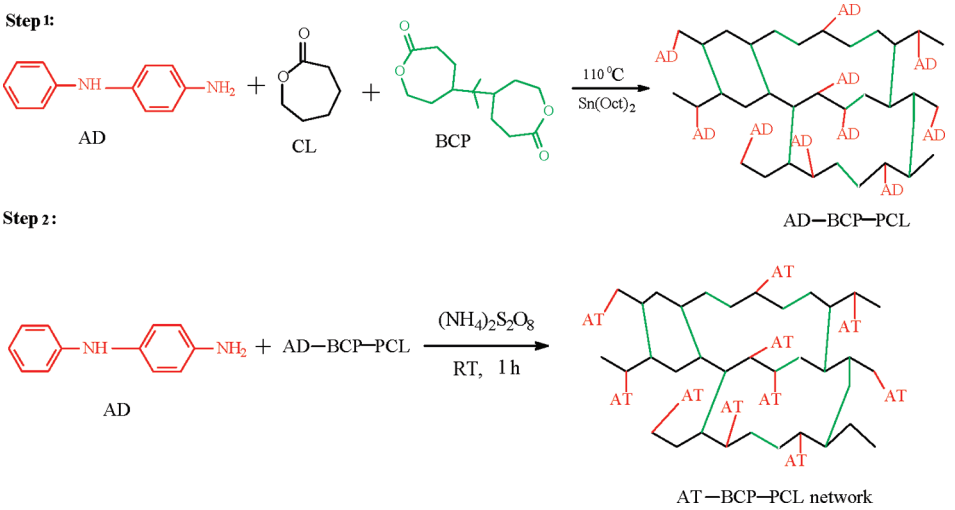

green and was vigorously stirred for 1 h at room temperature in the air. The mixture was filtered and the cake was washed by 50 mL acetone and 1 mol/L HCl mixture, and then 100 mL distilled water. The AT10—PCL polymer was dedoped in 0.1 mol/L NH_4OH solution for 10 min and the polymer was collected by filtration, and washed with distilled water until the filtrate was neutral. The polymer obtained was dried in a vacuum oven for 48 h. : ^{1}H NMR for AT15—PCL (400 MHz, DMSO-d_6): 9.95 (s, 1H, —CO—NH—), 9.61 (s, 1H, —CO—NH—), 8.46 (s, 1H, —NH—), 8.39 (s, 1H, —NH—), 7.77—6.67 (m, 13H, Ar—H), 4.36 (t, 2H, —CO—CH_2—), 3.98 (m, 2H, —O—CH_2), 2.27 (m, 2H, —CH_2—), 1.52 (m, 2H, —CH_2—), 1.28 (m, 2H, —CH_2—). ^{1}H NMR for AT15—PCL (400 MHz, $CDCl_3$): 4.03 (m, 2H, —CH_2—), 3.64 (m, 2H, —CH_2OH), 2.32 (m, 2H, —CH_2—), 1.63 (m, 2H, —CH_2—), 1.37 (m, 2H, —CH_2—).

Synthesis of AD—BCP—PCL and AT—BCP—PCL Organogels. The synthesis of the cross-linked network of the polymers was carried out in a manner similar to that of the AT—PCL block copolymers, as shown in Scheme 2. The difference was that the appropriate amount of cross-linker BCP was added to the AD and CL mixture in the first step (Table 1). The AD—BCP—PCL organogel was obtained after the reaction and the AT—BCP—PCL organogel was prepared by postfunctionalization with AD in a manner similar to the synthesis of AT—PCL. Five mL DMF and 10 mL acetone mixture was also used as solvent.

Characterization. The FT-IR spectrum of the copolymer was recorded on a PerkinElmer Spectrum 2000 FT-IR equipped with an attenuated total reflectance crystal accessory (Golden Gate) in the 4000—600 cm^{-1} range. The spectrum was based on 20 scans at 4 cm^{-1} resolution with a correction for atmospheric moisture and carbon dioxide.

The ^{1}H NMR (400 MHz) spectrum of the polymer was obtained using a Bruker Avance NMR instrument, $CDCl_3$ and DMSO-d_6 being used as the solvents for the samples and internal standards (δ = 7.26 ppm for $CDCl_3$, and δ = 2.50 ppm for DMSO-d_6). Approximately 10 mg of sample was dissolved in 1 mL solvent in a 5 mm sample tube.

Size exclusion chromatography (SEC) was used to determine the molecular weights (M_n) and molecular weight distribution (MWD) of the polymers. SEC was carried out using a TDA Model 301 equipped with one or two GMH_{HR}-M columns with TSK-gel (Tosoh Biosep), a VE 5200 GPC Autosampler, a VE 1121 GPC solvent pump and a VE 5710 GPC degasser, all of which were from Viscotek Corp. Tetrahydrofuran was used as the mobile phase (flow rate 1.0 mL/min). The measurement was performed at 35 °C. A conventional calibration was carried out using narrow linear polystyrene standards.

dx.doi.org/10.1021/ma2009595 |*Macromolecules* 2011, 44, 5227–5236

The UV−vis spectra of AD, AT, AD−PCL, and AT−PCL in DMSO solutions were recorded on a UV−vis spectrophotometer (UV-2401).

The thermal properties of the polymers were investigated using Differential Scanning Calorimetry (DSC, Mettler Toledo DSC 820 module) under a nitrogen atmosphere (nitrogen flow rate of 50 mL/min). The specimens were heated to 100 °C and then cooled to −70 °C to erase the thermal history of the polymers. The second scan from −70 to +100 °C at 10 °C/min was used to record the heat of fusion. The crystallization temperature (T_c) and melting temperature (T_m) were obtained from the second heating scan. The crystallinity (X_c) was calculated as: $X_c=\Delta H_f/\Delta H_f^0$, where ΔH_f is the enthalpy of fusion of the sample, and ΔH_f^0 is the enthalpy of fusion of a 100% crystalline PCL. The value for ΔH_f^0 of the PCL used for the calculations was 139.5 J/g.[35]

The thermal stability and composition of the copolymers were evaluated by thermogravimetric analysis (TGA) using a Mettler-Toledo TGA/SDTA 851^e module under a nitrogen atmosphere (nitrogen flow rate 50 mL/min) with a sample mass of 10 ± 1 mg and a heating rate of 10 °C/min. The scan range was from 50 to 800 °C.

Cyclic voltammetry (CV) of the AD−PCL and AT−PCL polymers was performed on an Electrochemical Workstation interfaced and monitored with a PC computer. A three-electrode system, i.e. a platinum disk as working electrode (surface area 0.14 cm^2), a platinum-wire as auxiliary electrode, and an Ag/AgCl as reference electrode, was employed. The 20 mg sample was dissolved in 6 mL DMSO, and was then doped with 0.2 mL 1 mol/L HCl. The mixture was deoxygenated for 10 min with nitrogen prior to the electrochemical measurements. The scan rate was set as 40 mV/s for all the samples.

AT−PCL polymers and AT−BCP−PCL organogels were dissolved or swollen in $CHCl_3$ and then doped with the same amount of 1 mol/L HCl. These polymers/organogels after doping were dried in the vacuum oven for 3 day and there should be no solvent in the polymers and organogels. The pellets of the polymers and organogels were obtained in a compression mold equipment at 35 °C under a pressure of 50 kN/m^2 for 1 min. The electrical conductivity of the copolymer and organogel pellets was determined by the standard Van Der Pauw four−probe method.

RESULTS AND DISCUSSION

Synthesis of Degradable and Electroactive Polymers and Organogels. Conductive segments and degradable segments were separately synthesized, and they were then connected together by chemistry reaction to prepare degradable and conductive polymers in all the previous work. There are several limitations concerning this strategy, such as multiple step reaction and low efficiency. Here, we demonstrate a universal two-step reaction to synthesize a series of degradable and electroactive block copolymers and organogels based on polyester and aniline oligomer. Polyesters obtained by ROP of lactones and lactides usually have a tailored molecular structure and specific end groups.[1,13] We used AD to initiate the ROP of CL with $Sn(Oct)_2$ as catalyst in bulk, since AD with a low molecular weight can dissolve in CL. This avoids the use of an organic solvent in the polymerization. Thus, diblock copolymers AD−PCL with a controlled structure and molecular weight were formed with a rigid AD segment at the chain end as one block and the long degradable flexible PCL as the other block. This AD group in the polyesters was used for postpolymerization modification using an oxidative coupling reaction with AD, and an AT segment was formed at the chain end of the macromolecules (Scheme 1). The oxidative coupling of AD−PCL into AT−PCL polymers was carried out in an acid medium. Because of the hydrophobic nature of the PCL segments, the subsequent purification by filtration was quite easy, and the yield of the product was quite high. If BCP cross-linker was added in the first step, a cross-linked degradable and electroactive organogel was formed (Scheme 2). The polymers obtained by Scheme 2 cannot dissolve in chloroform, and can just swell in chloroform. This is different from that of AT−PCL copolymers which can easily dissolve in $CHCl_3$. This is the direct evidence of the formation of the organogel. The chemical structures of the polymers obtained were investigated by FT-IR and NMR.

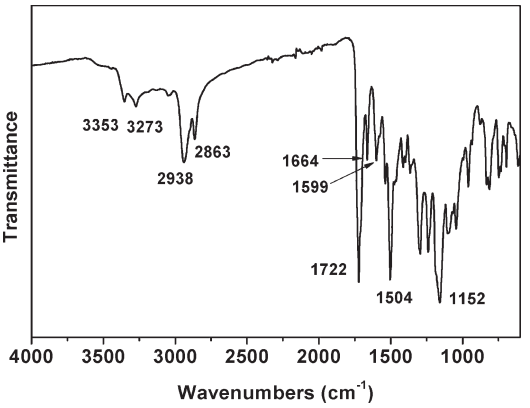

Figure 1. FT-IR of AT10−PCL.

A representative FT-IR spectrum of AT10−PCL is shown in Figure 1. The absorbance peaks at 1722 and 1152 cm^{-1} correspond to the −CO− ester group and −C−O−C− group in PCL segments. The peaks at 2938 and 2863 cm^{-1} are assigned to the $-CH_2-$ groups in PCL. The absorption peak of the amide group (−CO−NH−) appeared at 1664 cm^{-1}, indicating that the ring-opening polymerization of CL initiated by amine group of AD has taken place. The peaks at 1599 and 1504 cm^{-1} are attributed to the characteristic absorption of the quinone ring and benzene ring in the AT segment, respectively. These results demonstrated that the AT−PCL copolymer was formed.

The copolymer was further characterized by NMR spectra, and the results are shown in Figure 2. The peak of the amine group ($-NH_2$) appeared at 4.79 ppm in the ^1H NMR spectrum of AD in Figure 2A. Such peak was absent in Figure 2B for AD−PCL, but a new peak is present at 9.70 ppm corresponding to an amide group formed during the ring-opening polymerization of monomer CL initiated by the amine group of AD. In addition, there is a new peak at 4.36 ppm assigned to $-CH_2-$ group that connected to the amide group, which further demonstrated that the ROP of CL initiated by AD has taken place. The integral of the peak of $-CH_2-$ at 4.36 ppm is almost twice as large as that of the peak at 9.70 ppm. This is also consistent with the chemical structure of AD−PCL. In Figure 2C for AT−PCL, the characteristic peak of the amide group appeared at 9.95 and 9.61 ppm, and the imine group −NH− in the AT segment in the copolymer also showed two peaks at 8.46 and 8.39 ppm,[36] probably because there may be a position isomer and cis/trans isomer of AT in solution.[37] The peak at 7.99 ppm in Figure 2B assigned to the −NH− group is completely absent in Figure 2C, indicating that all the AD−PCL copolymers were transferred to AT−PCL copolymers. This demonstrates the high efficiency of the oxidative coupling reaction between AD and AD segments in the copolymers. There is no peak around 5.5 ppm corresponding to the $-NH_2$ group of AT segment in Figure 2C, indicating that no free AT segment was formed during the oxidative coupling of AD with AD−PCL.[28,38]

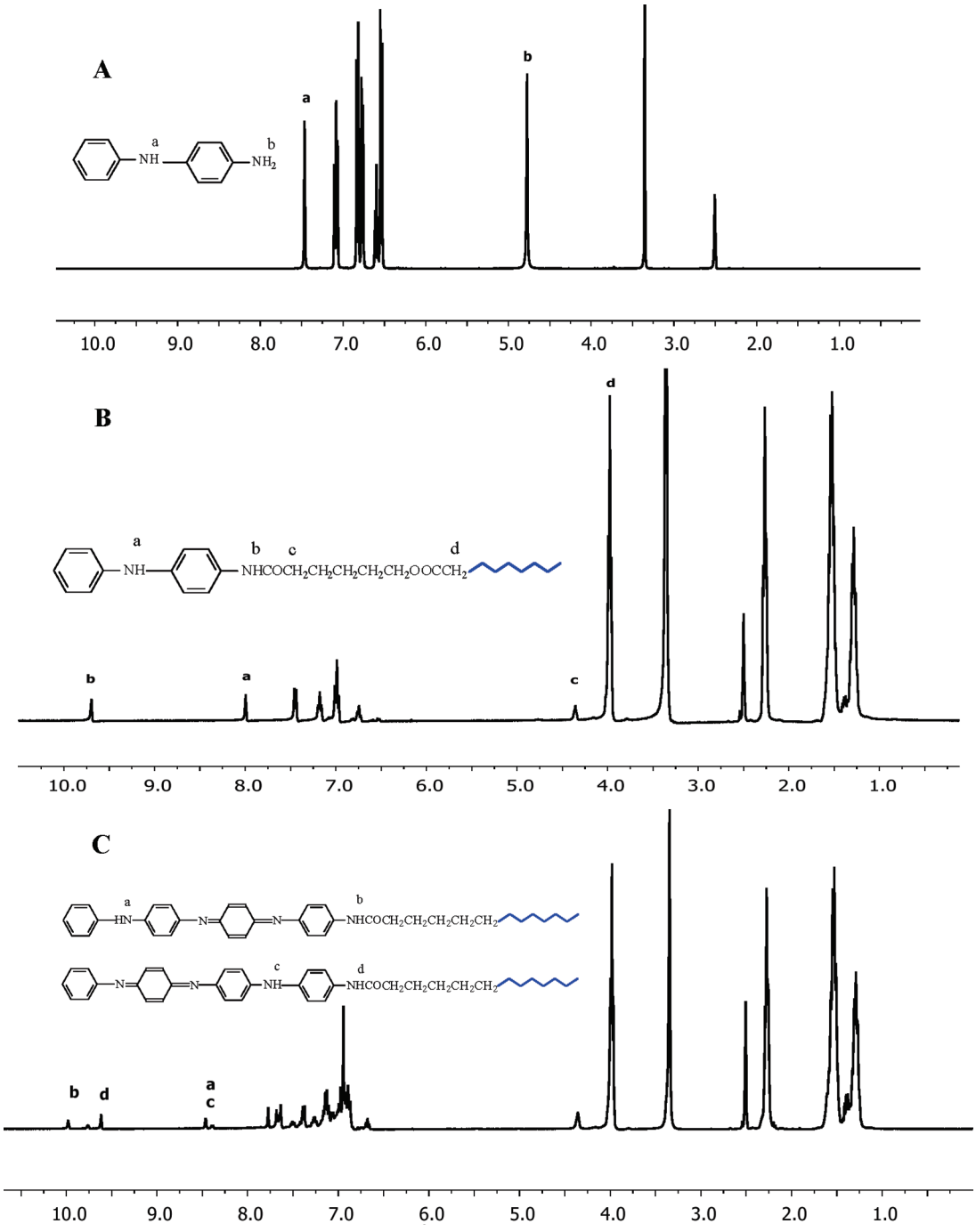

Figure 2. ^{1}H NMR spectra of (A) AD, (B) AD20−PCL, and (C) AT20−PCL in DMSO-d_6.

NMR spectrum was also used to calculate the monomer conversion and molecular weights of the block copolymers. Monomer conversion in the ROP of CL was calculated by comparing the integral of peak of methylene protons in PCL at δ = 3.98 ppm in Figure 2B with those of monomer CL at δ = 4.20 ppm, and the results are listed in Table 2. The monomer conversion of all the systems exceeded 98% after 48 h. The molecular weights of the block copolymers were determined by comparing the peak integrals of methylene $-CH_2-$ protons at δ = 4.03 ppm with those of the methylene protons next to the terminal hydroxyl groups $-CH_2OH$ at δ = 3.64 ppm[27] in Figure 3 (also see Figure 2 in Supporting Information). The NMR results are listed in Table 2. These results are very close to the theoretical ones. All these results indicate the successful synthesis of the AT−PCL copolymers.

The SEC curves of the AD−PCL and AT− PCL polymers are shown in Figure 4. There is only a single symmetric peak for all the polymers. The molecular weights from NMR results agreed very well with the molecular weights from SEC as shown in Table 2. Theoretically, the molecular weight of an AT−PCL copolymer increases by 184 when the corresponding AD−PCL polymer is coupled with AD. The molecular weights of AT−PCL

dx.doi.org/10.1021/ma2009595 |*Macromolecules* 2011, 44, 5227–5236

Table 2. Properties of the AD−PCL and AT−PCL block copolymers

sample code	reaction time (h)	monomer conversion[a] (%)	M_n[b] (g/mol)	M_n[c] (g/mol)	MWD[c]	M_n theory[d] (g/mol)
AD7.5−PCL	48	99	2500	2550	2.3	2450
AD10−PCL	48	98	1900	2000	2.2	1850
AD15−PCL	48	98	1400	1450	1.7	1250
AD20−PCL	48	99	950	1150	1.7	950
AT7.5−PCL			2900	2800	2.2	2650
AT10−PCL			2050	2100	2.0	2050
AT15−PCL			1500	1600	1.7	1400
AT20−PCL			1150	1300	1.5	1100

[a] Calculated from ^{1}H NMR on crude reaction mixture. [b] Determined by ^{1}H NMR. [c] Determined by SEC. [d] Theoretical number-average molecular weight, $M_n=[M]/[I]_{co} \times M_{CL} \times$ conversion.

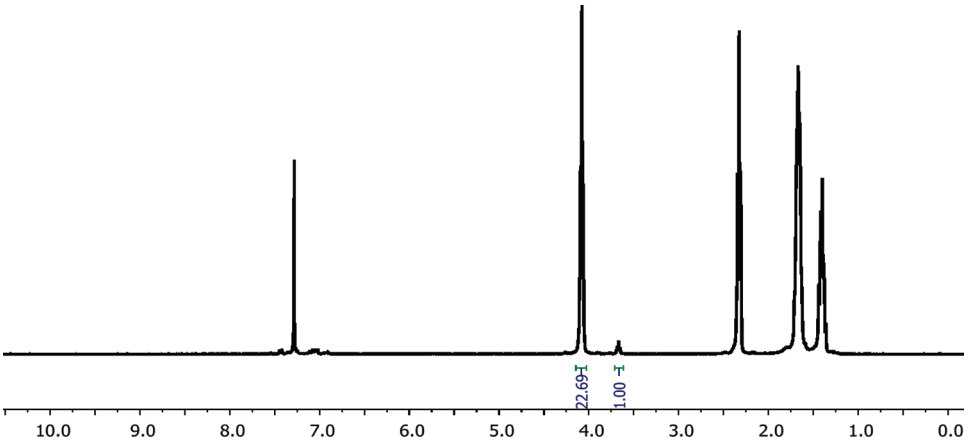

Figure 3. ^{1}H NMR spectrum of AT7.5−PCL in $CDCl_3$.

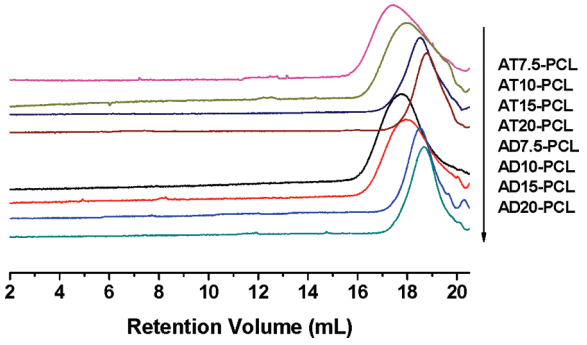

Figure 4. SEC curves of the AD−PCL and AT−PCL block copolymers.

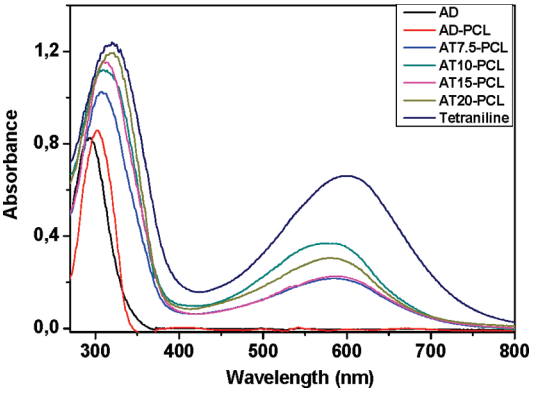

Figure 5. UV spectra of AD, AT, AD−PCL, and AT−PCL polymers in DMSO.

polymers obtained from both NMR and SEC increased by around 200 compared to that of the corresponding AD−PCL polymers, which indicates that the AT−PCL was successfully synthesized. The MWD also became narrower compared to that of AD−PCL. More important, this indicates that the PCL segment was not degraded during the oxidative coupling reaction in acid medium. This means that the coupling reaction in acid solution can be used for the synthesis of degradable and electroactive polymers.

Electrochemical Properties of the Polymers. The electrochemical properties of the polymers were characterized by UV absorption and cyclic voltammetry. The UV spectra of AD, AT, AD−PCL, and AT−PCL in DMSO are shown in Figure 5. The UV spectrum of AD exhibits an absorption peak at 294 nm, which is assigned to the absorption of the benzene ring. The AD−PCL shows a single peak at a higher wavelength at 302 nm, and this is also attributed to the absorption of the benzene ring in AD−PCL. This absorption shift can be explained by the fact that the amide group formed from the amine group of AD and PCL presumably conjugates with the benzene ring to form a longer conjugated system. The UV spectra of AT7.5−PCL, AT10−PCL, AT15−PCL, and AT20−PCL both showed two absorption peaks at about 306−319 and 580 nm, which are attributed to the $\pi-\pi^*$ transition of the benzene ring and the benzenoid (B)

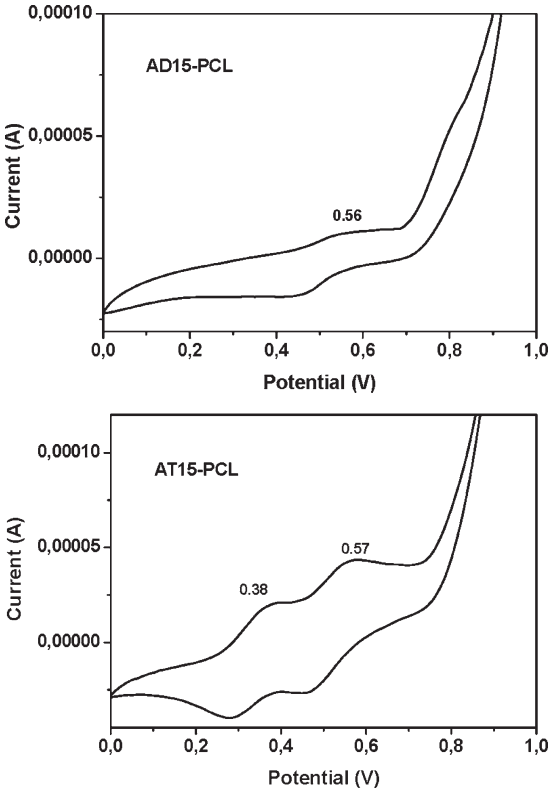

Figure 6. Cyclic voltammograms of the AD15−PCL and AT15−PCL block copolymers.

to quinoid (Q) $\pi_B-\pi_Q$ excitonic transition.[39] It was found that the benzene ring absorption of AT7.5−PCL, AT10−PCL, AT15−PCL, and AT20−PCL appeared at 306, 309, 311, and 319 nm, respectively, and the peaks showed a shorter wavelength than that of AT at 321 nm. The benzenoid absorption region indicates the effective conjugation length of the conjugated system,[22] and we consider that this blue shift may be because the long and flexible PCL chains restrict the nonplanar conformation of the AT segments, resulting in a decrease in the effective conjugation length of AT in the copolymer. Furthermore, compared with the Q/B intensity ratio of pure AT, the ratio of the AT−PCL sample was much lower and showed an obvious blue shift, which is probably because the amide group −NH−CO− is an electron-withdrawing group compared to $-NH_2$, which decreases the electronic concentration of the quinone units.[40]

Figure 6 shows the cyclic voltammograms (CV) of the AD15−PCL and AT15−PCL polymers. There is one pair of oxidation/reduction peaks at 0.56 V for AD15−PCL, which is assigned to the transition from the leucoemeraldine state to the emeraldine state of AD segment as shown in Scheme 3. In the case of the AT15−PCL polymer, two pairs of well-defined oxidation/reduction peaks appeared at 0.38 and 0.57 V in the CV. The peak at 0.38 V is assigned to the transition from the leucoemeraldine state to the emeraldine state. At a higher potential, 0.57 V, the AT segment in the polymer was oxidized from the emeraldine state to the pernigraniline state. The proposed mechanism for the molecular changes of AT15−PCL is also shown in Scheme 3. This confirmed that the AT segment was formed during the coupling reaction of AD−PCL with AD. Our CV results for AT15−PCL with AT segments are consistent with our previous result[28] and other references.[41,42] All these results from the UV spectra and CVs demonstrated that these AT−PCL polymers have good electroactivity.

Conductivity of the Polymers. The electrical conductivities of the AT−PCL polymers and AT−BCP−PCL organogels were tested on their compressed films using a standard four probe technique, and the data are listed in Table 3. We found that the electrical conductivity of the AT−PCL polymers in the range of 6.30×10^{-7} S/cm and 1.03×10^{-5} S/cm increased with increasing AT content in the polymer. This is because there is an increasing chance of better $\pi-\pi$ stacking of the AT segment with increasing AT content in the matrix and this favors hopping. However, these conductivity values are lower than that of pure AT, due to the nonconductive PCL incorporated into the matrix. On the other hand, these AT−PCL block copolymers formed self-assembly aggregates with the conductive AT segment as core and the PCL segment as shell, which was confirmed by the ^{1}H NMR spectrum of the AT−PCL copolymer in $CDCl_3$, since there is no peak corresponding to the AT segment, as shown in Figure 3 (also see Figure 2 in the Supporting Information). The microseparation occurred as a result of a self-assembly process.[22] The conductive AT domains were separated by the continuous nonconductive PCL matrix. Consequently, the conductivity of the AT−PCL polymers was achieved by a tunnel effect through the PCL matrix between the two neighboring conductive domains. For these reasons, the conductivity of AT−PCL polymers was much lower than that of AT. However, this conductivity is adequate for biomedical applications, since the in vivo microcurrent is usually very low,[43] and the conductivity of the copolymers is over a wide range tuned by the AT content, and this could be utilized for specific biomedical applications.

In the case of the AT−BCP−PCL organogels, the conductivity test could only be applied to the AT7.5−BCP−PCL pellets. The AT−BCP−PCL organogels cannot crystallize due to their cross-linked structure, and the organogels are in a rubbery state. So that the pellets of these organogels are compressed then tend to recover. As a result, the thickness and density of these pellets are not uniform. The conductivity of AT7.5−BCP−PCL organogel was 7.40×10^{-7} S/cm, which is higher than that of AT7.5−PCL, probably due to the network effect.

Thermal Properties of the Polymers. The thermal properties of the electroactive polymeric materials are also very important for their applications. The thermal stability of these block copolymers and organogels was tested by TGA, and their thermalgrams are shown in Figure 7. The thermal degradation of the AD−PCL polymers clearly exhibits a two-step behavior. There is an evident weight loss for the AD−PCL series of polymers when the temperature was raised from 150 to 410−430 °C, attributed to the degradation of the less thermally stable PCL segments. When the temperature was raised above 410−430 °C, there was a second weight loss between 410−430 and 620 °C, and 7.5% to 20% of the weight ratio of the copolymers was lost depending on the AD content of the block copolymers, corresponding to the degradation of the AD segments. The AD−PCL copolymers exhibited a greater thermal stability with increasing AD content in the polymer, due to the better thermal stability of the AD segment. The thermal degradation of the AT−PCL was similar to that of the AD−PCL polymers, but the AT−PCL polymers had a greater thermal stability than the corresponding AD−PCL polymers, because the AT−PCL polymers have a higher content of AT than the content of AD in the AD−PCL polymers. The AT contents in the AT−PCL polymers were calculated from the TGA curves from the second degradation stage, and the results

Scheme 3. Molecular Changes in the AD−PCL and AT−PCL at Different Oxidation States

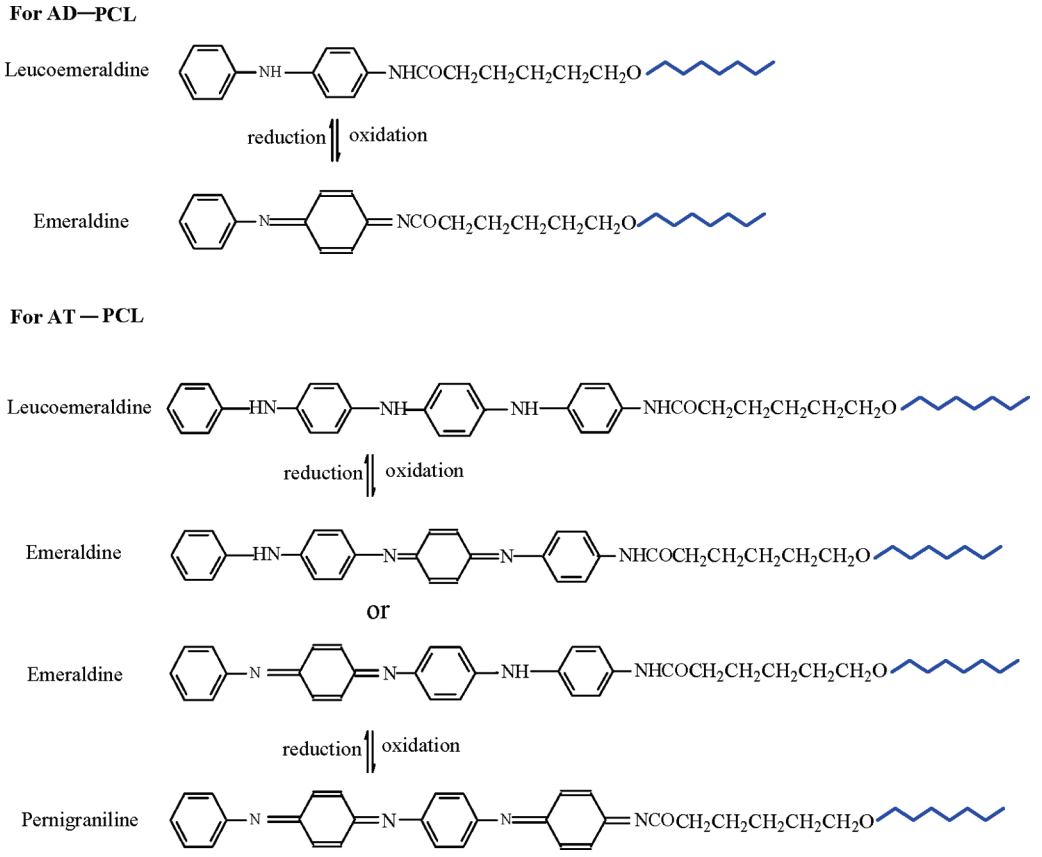

Table 3. Conductivity and AT Content of the Polymers and Organogels

sample code	conductivity (S/cm)	% AT content from TGA (theoretical)
AT7.5−PCL	6.30×10^{-7}	15 (13.8)
AT10−PCL	2.08×10^{-6}	20 (17.9)
AT15−PCL	5.33×10^{-6}	27 (26.2)
AT20−PCL	1.03×10^{-5}	32 (33.3)
AT7.5−BCP−PCL	7.40×10^{-7}	17 (13.8)

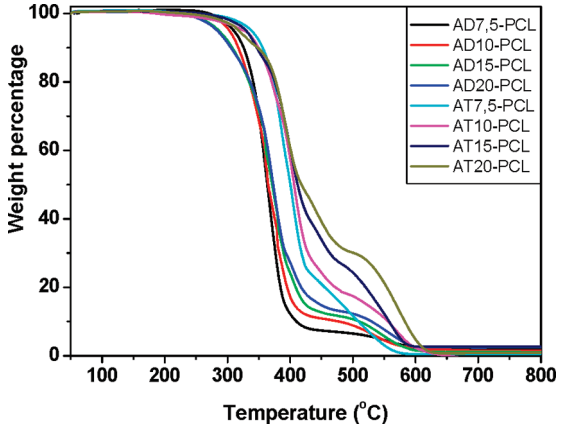

Figure 7. TGA thermograms of AD−PCL and AT−PCL block copolymers.

are listed in Table 3. These values are close to the theoretical contents, confirming the successful synthesis of the AT−PCL block copolymers. The thermal degradation behavior of the AD−BCP−PCL and AT−BCP−PCL organogels was similar to that of the AD−PCL and AT−PCL polymers (see Figure 3 in the Supporting Information).

The crystallization temperature (T_c), melting temperature (T_m), and crystallinity (X_c) of the polymers and organogels were determined by DSC. The DSC curves of AD10−PCL, AT10−PCL, AD10−BCP−PCL, and AT10−BCP−PCL are shown in Figure 8, and the data are listed in Table 4. It is evident that the X_c decreased with increasing AD content in the AD−PCL block copolymers, probably because the rigid AD segment restricts to some extent the motion of the flexible PCL segment, which impedes the crystallization process, and leads to imperfect crystallization. Because of the lower crystallinity and the imperfection of the crystallization, the T_m of the AD−PCL polymers decreased with increasing AD content or with decreasing molecular weight of the polymer. The T_c was used to evaluate the nucleation during polymer melt crystallization. The crystallizing ability of the polymer increased with increasing T_c.[44] The T_c of the AD−PCL polymers also decreased with increasing AD content. The T_c of AD15−PCL and AD20−PCL polymers decreased particularly dramatically, probably because the high content of the rigid AD segment

dx.doi.org/10.1021/ma2009595 |Macromolecules 2011, 44, 5227–5236

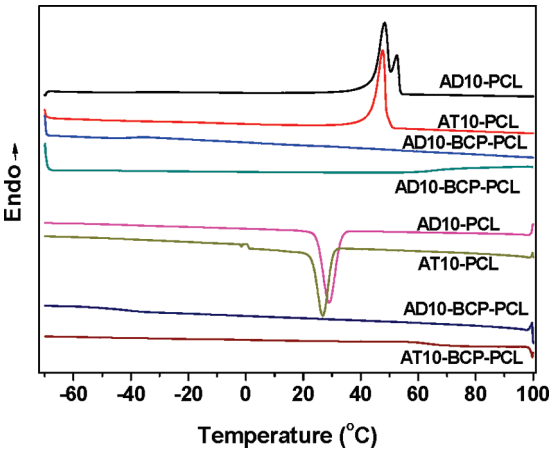

Figure 8. DSC curves of the polymers and organogels.

Table 4. T_c, T_m, and X_c of the Polymers

sample code	T_c (°C)	T_m (°C)	X_c
AD7.5−PCL	29.4	54.2	47.8
AD10−PCL	29.1	48.2	43.1
AD15−PCL	20.8	41.9	38.7
AD20−PCL	8.0	37.8	33.0
AT7.5−PCL	29.2	53.4	42.0
AT10−PCL	26.9	47.5	32.5
AT15−PCL	17.0	41.0	24.8
AT20−PCL	−1.9	36.7	4.4

strongly hindered the crystallization and lowered the crystallizing ability of the polymers.

The trend of T_c, T_m, and X_c for the AT−PCL copolymers was similar to that for the AD−PCL polymers; i.e. the T_c, T_m, and X_c decreased with increasing AT content. The T_c, T_m, and X_c of the AT−PCL polymers were lower than the values for the corresponding AD−PCL polymers, because the length of the rigid AT segment is much longer than that of the AD segment, and the content of AT in the AT−PCL polymers is much higher than the content of AD in the AD−PCL polymers. For these two reasons, the crystallization of the AT−PCL polymers was more disturbed than that of the AD−PCL polymers.

In the case of the AD−BCP−PCL and AT−BCP−PCL organogels, there was no crystallization during the heating and cooling cycles as shown in Figure 8, because the cross-linked network prevented the movement of chain segments into the lattice. This confirmed that the AD−BCP−PCL and AT−BCP−PCL organogels were indeed cross-linked by BCP. These thermal properties of the polymers and organogels further verified their chemical structures.

In contrast to the previous complex and multiple step reaction to synthesize degradable and electroactive polymers, our synthesis strategy of well-defined structured diblock copolymers and organogels is a two-step and universal approach, and this facile route will lead to a library of degradable and electroactive block copolymers and networks based on aniline oligomer and polyesters, such as polylactide, polycaprolactone, poly(1, 5-dioxepan-2-one), poly(trimethylene carbonate), and so on.

CONCLUSION

A universal two-step strategy for the synthesis of degradable and electroactive block copolymers and networks (DEBCNs) based on an aniline oligomer and polyesters has been described and performed. A series of degradable and electroactive diblock copolymers and networks based on aniline tetramer (AT) and PCL with tunable molecular weight and AT content have been simply prepared according to this new approach by controlled ring-opening polymerization (ROP) of ε-caprolactone and a postpolymerization functionalization via an oxidative coupling reaction. FT-IR, NMR and SEC spectra have verified the well-defined structure of the block copolymers. UV and CV results have demonstrated the excellent electroactivity of the polymers, and the conductivity of the polymers between 6.30×10^{-7} S/cm and 1.03×10^{-5} S/cm was tuned by the AT content. The thermal properties obtained from TGA and DSC data are consistent with the chemical structures of the diblock copolymers and organogels. This approach to combine ROP and postfunctionalization is a simple procedure for the synthesis of DEBCNs, and these DEBCNs with well-defined structures and properties offer new possibilities in biomedical applications such as neural and cardiac regeneration where the electroactivity is needed.

ASSOCIATED CONTENT

Supporting Information. ^{1}H NMR spectra of BCP and AT−PCL copolymers in $CDCl_3$, and TGA of AD−BCP−PCL and AT−BCP−PCL organogels. This material is available free of charge via the Internet at http://pubs.acs.org.

AUTHOR INFORMATION

Corresponding Author

*Telephone: +46-8-790 8274. Fax: +46-8-20 84 77. E-mail: aila@polymer.kth.se.

ACKNOWLEDGMENT

The authors acknowledge the China Scholarship Council (CSC) and The Royal Institute of Technology (KTH) for financial support for this work.

REFERENCES

(1) Albertsson, A. C.; Varma, I. K. *Biomacromolecules* **2003**, *4*, 1466–1486.

(2) Albertsson, A. C.; Varma, I. K. Aliphatic polyesters: Synthesis, properties and applications. *Adv. Polym. Sci.* **2002**, *157*, 1–40.

(3) Stridsberg, K. M.; Ryner, M.; Albertsson, A. C. Controlled ring-opening polymerization: Polymers with designed macromolecular architecture. *Adv. Polym. Sci.* **2002**, *157*, 41–65.

(4) Ryner, M.; Finne, A.; Albertsson, A. C.; Kricheldorf, H. R. *Macromolecules* **2001**, *34*, 7281–7287.

(5) Dechy-Cabaret, O.; Martin-Vaca, B.; Bourissou, D. *Chem. Rev.* **2004**, *104*, 6147–6176.

(6) Kowalski, A.; Libiszowski, J.; Biela, T.; Cypryk, M.; Duda, A.; Penczek, S. *Macromolecules* **2005**, *38*, 8170–8176.

(7) You, Z. W.; Cao, H. P.; Gao, J.; Shin, P. H.; Day, B. W.; Wang, Y. D. *Biomaterials* **2010**, *31*, 3129–3138.

(8) Chen, W.; Yang, H. C.; Wang, R.; Cheng, R.; Meng, F. H.; Wei, W. X.; Zhong, Z. Y. *Macromolecules* **2010**, *43*, 201–207.

(9) Plikk, P.; Tyson, T.; Finne-Wistrand, A.; Albertsson, A. C. *J. Polym. Sci., Part A: Polym. Chem.* **2009**, *47*, 4587–4601.

(10) Edlund, U.; Kallrot, M.; Albertsson, A. C. *J. Am. Chem. Soc.* **2005**, *127*, 8865–8871.
(11) Finne, A.; Albertsson, A. C. *J. Polym. Sci., Part A: Polym. Chem.* **2004**, *42*, 444–452.
(12) Malberg, S.; Plikk, P.; Finne-Wistrand, A.; Albertsson, A. C. *Chem. Mater.* **2010**, *22*, 3009–3014.
(13) Srivastava, R. K.; Albertsson, A. C. *Macromolecules* **2006**, *39*, 46–54.
(14) Mahmud, A.; Xiong, X. B.; Lavasanifar, A. *Macromolecules* **2006**, *39*, 9419–9428.
(15) Korich, A. L.; Walker, A. R.; Hincke, C.; Stevens, C.; Iovine, P. M. *J. Polym. Sci., Part A: Polym. Chem.* **2010**, *48*, 5767–5774.
(16) Hench, L. L.; Polak, J. M., *Science* **2002**, *295*, 1014-+.
(17) Wong, J. Y.; Langer, R.; Ingber, D. E. *Proc. Natl. Acad. Sci. U.S.A* **1994**, *91*, 3201–3204.
(18) Guimard, N. K.; Gomez, N.; Schmidt, C. E. *Prog. Polym. Sci.* **2007**, *32*, 876–921.
(19) Zelikin, A. N.; Lynn, D. M.; Farhadi, J.; Martin, I.; Shastri, V.; Langer, R. *Angew. Chem., Int. Ed.* **2002**, *41*, 141–144.
(20) Rivers, T. J.; Hudson, T. W.; Schmidt, C. E. *Adv. Funct. Mater.* **2002**, *12*, 33–37.
(21) Guimard, N. K. E.; Sessler, J. L.; Schmidt, C. E. *Macromolecules* **2009**, *42*, 502–511.
(22) Huang, L. H.; Hu, J.; Lang, L.; Wang, X.; Zhang, P. B.; Jing, X. B.; Wang, X. H.; Chen, X. S.; Lelkes, P. I.; MacDiarmid, A. G.; Wei, Y. *Biomaterials* **2007**, *28*, 1741–1751.
(23) Huang, L. H.; Zhuang, X. L.; Hu, J.; Lang, L.; Zhang, P. B.; Wang, Y. S.; Chen, X. S.; Wei, Y.; Jing, X. B. *Biomacromolecules* **2008**, *9*, 850–858.
(24) Zhang, Q. S.; Yan, Y. H.; Li, S. P.; Feng, T. *Biomed. Mater.* **2009**, *4*, No. article no. 035008.
(25) Zhang, Q. S.; Yan, Y. H.; Li, S. P.; Feng, T. *Mater. Sci. Eng., C* **2010**, *30*, 160–166.
(26) Guo, B. L.; Finne-Wistrand, A.; Albertsson, A. C. *Biomacromolecules* **2010**, *11*, 855–863.
(27) Guo, B. L.; Finne-Wistrand, A.; Albertsson, A. C. *Macromolecules* **2010**, *43*, 4472–4480.
(28) Guo, B. L.; Finne-Wistrand, A.; Albertsson, A. C. *Chem. Mater.* **2011**, *23*, 1254–1262.
(29) Guo, B. L.; Finne-Wistrand, A.; Albertsson, A. C. *J. Polym. Sci., Part A: Polym. Chem.* **2011**, *49*, 2097–2105.
(30) Guo, B. L.; Finne-Wistrand, A.; Albertsson, A. C. *Biomacromolecules* **2011**10.1021/bm200389t.
(31) Ding, C. F.; Wang, Y.; Zhang, S. S. *Eur. Polym. J.* **2007**, *43*, 4244–4252.
(32) Hu, J.; Huang, L. H.; Zhuang, X. L.; Zhang, P. B.; Lang, L.; Chen, X. S.; Wei, Y.; Jing, X. B. *Biomacromolecules* **2008**, *9*, 2637–2644.
(33) Andronova, N.; Srivastava, R. K.; Albertsson, A. C. *Polymer* **2005**, *46*, 6746–6755.
(34) Palmgren, R.; Karlsson, S.; Albertsson, A. C. *J. Polym. Sci., Part A: Polym. Chem.* **1997**, *35*, 1635–1649.
(35) Andronova, N.; Finne, A.; Albertsson, A. C. *J. Polym. Sci., Part A: Polym. Chem.* **2003**, *41*, 2412–2423.
(36) Kim, H.; Park, J. W. *J. Mater. Chem.* **2010**, *20*, 1186–1191.
(37) MacDiarmid, A. G.; Zhou, Y.; Feng, J. *Synth. Met.* **1999**, *100*, 131–140.
(38) Rozalska, I.; Kulyk, P.; Kulszewicz-Bajer, I. *New J. Chem.* **2004**, *28*, 1235–1243.
(39) Chen, R.; Benicewicz, B. C. *Macromolecules* **2003**, *36*, 6333–6339.
(40) Guo, Y.; Mylonakis, A.; Zhang, Z. T.; Lelkes, P. I.; Levon, K.; Li, S. X.; Feng, Q. W.; Wei, Y. *Macromolecules* **2007**, *40*, 2721–2729.
(41) Chao, D. M.; Ma, X. B.; Liu, Q. H.; Lu, X. F.; Chen, J. Y.; Wang, L. F.; Zhang, W. J.; Wei, Y. *Eur. Polym. J.* **2006**, *42*, 3078–3084.
(42) Han, D. H.; Pan, C. Y. *Polymer* **2006**, *47*, 6956–6962.
(43) Niple, J. C.; Daigle, J. P.; Zaffanella, L. E.; Sullivan, T.; Kavet, R. *Bioelectromagnetics* **2004**, *25*, 369–373.
(44) Zhao, Y.; Keroack, D.; Prud'homme, R. *Macromolecules* **1999**, *32*, 1218–1225.